AIMS Mathematics

http://www.aimspress.com/journal/Math

AIMS Mathematics, 4(2): 316–326.
DOI:10.3934/math.2019.2.316
Received: 19 January 2019
Accepted: 26 March 2019
Published: 09 April 2019

Research article

Free surface flows over a successive obstacles with surface tension and gravity effects

Abdelkader Laiadi[1,*] **and Abdelkrim Merzougui**[2]

[1] Department of Mathematics, Biskra University, Biskra, Algeria
[2] Department of Mathematics, M'sila University, M'sila, Algeria

* **Correspondence:** Email: laiadhi_a@yahoo.fr.

Abstract: The problem of steady two-dimensional flow of a fluid of finite depth over a successive obstacles is considered. Both gravity and surface tension are taken into account in the dynamic boundary conditions. The fluid is assumed to be inviscid, incompressible and the flow to be irrotational. The flow is characterized by the two parameters, the Froude number Fr and the inverse Weber number δ. The fully non-linear problem is solved numerically by using the boundary integral equation technique. The numerical solutions for sub-critical ($Fr < 1$) and supercritical ($Fr > 1$) are presented for various values of Fr and δ. The effects of surface tension and gravity on the shape of the free surface are discussed, and solution diagrams for all flow regimes are presented.

Keywords: free-surface flow; potential flow; Weber number; surface tension; Froude number; integro-differential equation
Mathematics Subject Classification: 76B07, 65E05, 76M15

1. Introduction

Free-surface flow over a submerged obstacles is one of the well-known classical problem in fluid mechanics. Many researchers have investigated free surface flows over an obstacle for different bottoms topography, for examples, Forbes and Schwartz [13] used the boundary integral method to find fully non-linear solutions of subcritical and supercritical flows over a semi-circular obstacle. Supercritical and critical flows over a submerged triangular obstacle were investigated by Dias and Vanden-Broeck [11]. They employed a series truncation methods to calculate the solutions. Abd-el-Malek and Hanna [1] studied flow over a triangular obstacle by using the Hilbert method with gravity effect. When the fluid is subjected to the interaction of gravity and surface tension, in this case, the problem is generally difficult to solve. Forbes [12] was among the first to propose numerical solutions of non-linear flows over a semi-circular obstruction under the effect of gravity and surface

tension. Later, many authors have studied this problem, for example, Grandison [14], Vanden-Broeck [24]. In the case of flows over two obstacles, Pratt [23] investigated this problem experimentally and theoretically using weakly non-linear analysis. Later, Belward [3] computed numerical solutions of a critical flow for which the hydraulic fall occurred at the leftmost obstacle with downstream supercritical flow. Recently, Binder, Vanden-Broeck and Dias [9] showed that there exist two types of solution in subcritical flow regime, and one type in supercritical flow regime. This paper is concerned with the numerical calculations of flow of finite depth over a successive obstacles. The purpose of this work is to examine further flows with many obstacles in order to classify the possible solutions. The effects of surface tension and gravity are included in the boundary conditions, the problem is solved numerically by using the boundary integral equation methods. These methods are based on a reformulation of the problem as a system of non-linear integro-differential equations for the unknown quantities on the free surface. These equations are then discretized and the resultant non-linear algebraic equations is solved by iteration. Such boundary integral equation methods have been used extensively by many researchers [3, 4, 6, 7, 15, 17] and others. It is assumed that there is uniform flow far upstream where the flow approaches a uniform stream with constant velocity U and depth H (see Figure 1). The problem is characterized by the two parameters the Froude number Fr defined by

$$Fr = \frac{U}{\sqrt{gH}} \tag{1.1}$$

and the inverse Weber number δ where

$$\delta = \frac{T}{\rho U^2 H} \tag{1.2}$$

Here T is the surface tension, g is the gravity and ρ is the fluid density. When $Fr < 1$, the flow is called subcritical and for $Fr > 1$ the flow far upstream is called supercritical. In this work, we calculate waveless solutions for both supercritical and subcritical flows by introducing the effects of surface tension.

Formulation of the problem and numerical procedure are given in section 2 and section 3 respectively. In section 4 we discuss the numerical results of free surface flows over a successive triangular obstacles with different angles γ_i, $i = 1, ..., m-2$ and for various values of the two parameters Fr and δ. Solution diagrams for all flow regimes are presented.

2. Mathematical formulation

We consider steady two-dimensional potential free surface flows past a submerged obstacles at the bottom of a channel (see Figure 1). The flow is assumed to be inviscid and incompressible. Fluid domain is bounded below by a horizontal rigid wall A_0A_m and the successive obstructions forming the angles γ_i, $i = 1, ..., m-2$ with the horizontal, where $0 < |\gamma_i| < \frac{\pi}{2}$, and above by the free surface EF. Let us introduce Cartesian coordinates with the $x-$ axis along the bottom and the $y-$ axis directed vertically upwards, gravity g is acting in the negative $y-$direction. Let's introduce the velocity potential $\phi(x, y)$ and the stream function $\psi(x, y)$ by defining the complex potential function f as

$$f(x, y) = \phi(x, y) + i\psi(x, y) \tag{2.1}$$

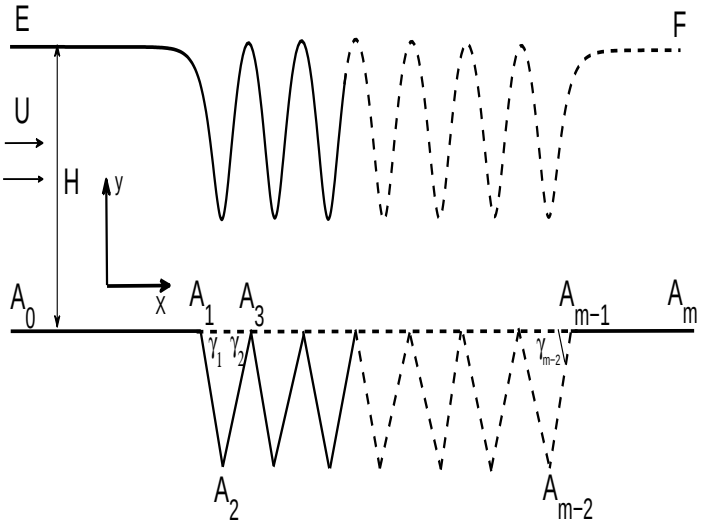

Figure 1. Sketch of the flows over a successive obstacles in the physical plane $z = x + iy$.

The complex velocity w can be written as

$$w = \frac{df}{dz} = u - iv \tag{2.2}$$

Here u and v are velocity components in the x and y directions, and $z = x + iy$. For convenience, we define dimensionless variables by taking H as the reference length and U as the reference velocity. Without loss of generality, we choose $\psi = 0$ on the free surface EF. By the choice of our dimensionless variables, we have $\psi = -1$ on the bottom A_0A_m and $\phi = 0$ at the point $A_{\frac{m}{2}}$ (see Figure 2).

The problem is formulated in terms of the velocity potential $\phi(x, y)$. This function satisfies Laplace's equation

$$\Delta\phi = 0 \quad \text{in the fluid domain}$$

The Bernoulli's equation on the free surface EF can be written

$$\frac{1}{2}\left(u^2 + v^2\right) + \delta K + \frac{1}{Fr^2}(y - 1) = \frac{1}{2}. \tag{2.3}$$

Here K is curvature of the free surface, Fr and δ are defined in (1.1) and (1.2) respectively.

The kinematic boundary conditions in f-plane are given by

$$\begin{cases} v = 0 \text{ on } \psi = -1 \text{ and } -\infty < \phi < \phi_{A_1} \text{ and } \phi_{A_{m-1}} < \phi < +\infty \\ v = u\tan|\gamma_i| \text{ on } \psi = -1 \text{ and } \phi_{A_i} < \phi < \phi_{A_{i+1}}, i = 1, ..., m-2 \end{cases} \tag{2.4}$$

Now we reformulate the problem as an integral equation. We define the function $\tau - i\theta$ by

$$w = u - iv = e^{\tau - i\theta} \tag{2.5}$$

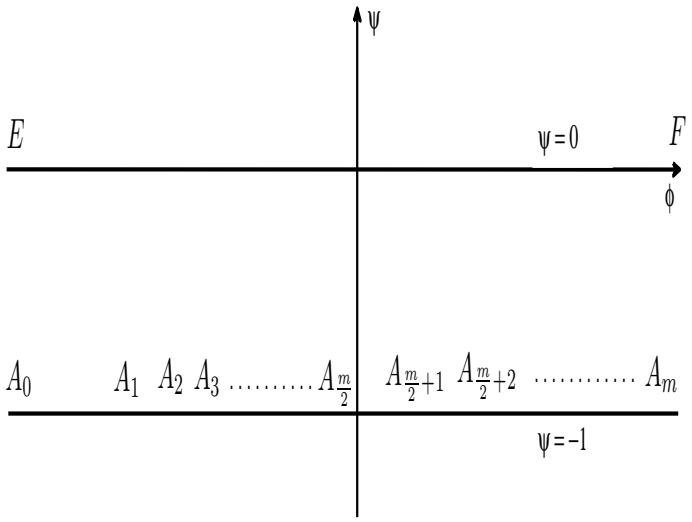

Figure 2. Sketch of the flow in the potential f-plane $f = \phi + i\psi$.

and we map the flow domain onto the upper half of the $\zeta-$plane by the transformation

$$\zeta = \alpha + i\beta = e^{-\pi f} = e^{-\pi\phi}\left(\cos\pi\psi - i\sin\pi\psi\right). \tag{2.6}$$

The flow in the $\zeta-$plane is shown in Figure 3. The curvature K of a streamline, in terms of θ, is

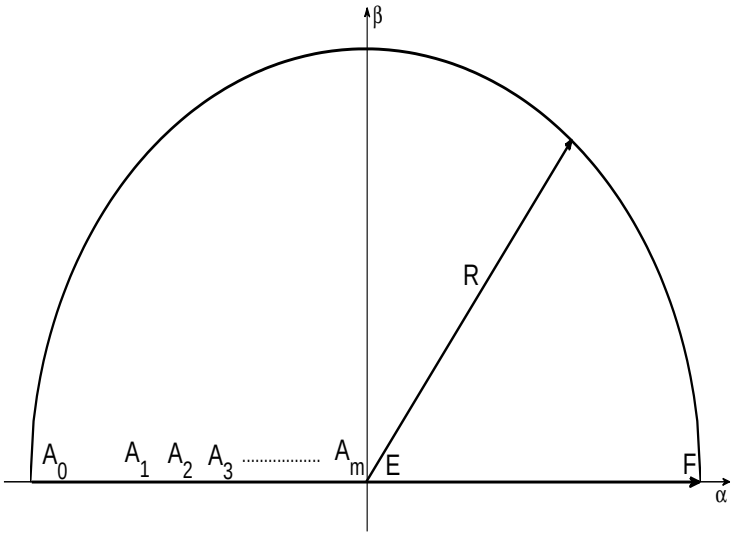

Figure 3. The upper half $\zeta-$plane $\zeta = \alpha + i\beta$.

given by

$$K = -e^{\tau}\left|\frac{\partial\theta}{\partial\phi}\right|. \tag{2.7}$$

Substituting (2.7) into (2.3), Bernoulli's equation becomes

$$\frac{1}{2}e^{2\tau} - \delta e^{\tau}\left|\frac{\partial\theta}{\partial\phi}\right| + \frac{1}{Fr^2}(y-1) = \frac{1}{2} \quad \text{on } EF. \tag{2.8}$$

We apply the Cauchy's integral formula to the function $\tau - i\theta$ in the complex ζ-plane with a contour consisting of the $\alpha-$axis and the semicircle of arbitrary large radius R in the upper half plane. After taking the real part and $R \longrightarrow +\infty$, we obtain

$$\tau(\alpha_0) = -\frac{1}{\pi}\int_{-\infty}^{+\infty}\frac{\theta(\alpha)}{\alpha-\alpha_0}d\alpha. \tag{2.9}$$

Where $\tau(\alpha_0)$ and $\theta(\alpha)$ denote the value of τ and θ on the free surface. The integral in (2.9) is a Cauchy principal value type.

The kinematic boundary conditions (2.4) in ζ-plane become

$$\begin{cases} \theta = 0 \quad \text{for } -\infty < \alpha < \alpha_{A_1} \quad \text{and } \alpha_{A_{m-1}} < \alpha < \alpha_{A_m} \\ \theta = \gamma_i \quad \text{for } \alpha_{A_i} < \alpha < \alpha_{A_{i+1}}, i = 1, ..., m-2 \\ \theta = \text{ unknown } \ 0 < \alpha < +\infty \end{cases} \tag{2.10}$$

By using (2.10), Eq (2.9) becomes :

$$\tau(\alpha_0) = -\frac{1}{\pi}\sum_{i=1}^{i=m-2}\gamma_i \log\left|\frac{\alpha_{A_{i+1}}-\alpha_0}{\alpha_{A_i}-\alpha_0}\right| - \frac{1}{\pi}\int_0^{+\infty}\frac{\theta(\alpha)}{\alpha-\alpha_0}d\alpha. \tag{2.11}$$

Rewriting this equation in terms of ϕ by substituting $\alpha = e^{-\pi\phi}$, $\alpha_0 = e^{-\pi\phi_0}$,

this gives

$$\tau'(\phi_0) = -\frac{1}{\pi}\sum_{i=1}^{i=m-2}\gamma_i \log\left|\frac{e^{-\pi\phi_{A_{i+1}}} + e^{-\pi\phi_0}}{e^{-\pi\phi_{A_i}} + e^{-\pi\phi_0}}\right| + \int_{-\infty}^{+\infty}\frac{\theta'(\phi)\,e^{-\pi\phi}}{e^{-\pi\phi} - e^{-\pi\phi_0}}d\phi. \tag{2.12}$$

Here $\tau'(\phi_0) = \tau(e^{-\pi\phi_0})$ and $\theta'(\phi) = \theta(e^{-\pi\phi})$. The Eq (2.8) is now rewritten in terms of τ' and θ' as

$$\frac{1}{2}e^{2\tau'(\phi_0)} - \delta e^{\tau'(\phi_0)}\left|\frac{\partial\theta'(\phi)}{\partial\phi}\right| + \frac{1}{Fr^2}(y-1) = \frac{1}{2} \quad \text{on } EF. \tag{2.13}$$

Integrating the identity

$$\frac{d(x+iy)}{df} = w^{-1}. \tag{2.14}$$

We obtain the following parametric representation of the free surface EF

$$x(\phi) = \int_{-\infty}^{\phi} e^{-\tau'(\phi_0)}\cos\theta'(\phi_0)d\phi_0 \quad \text{for } -\infty < \phi < +\infty \tag{2.15}$$

$$y(\phi) = 1 + \int_{-\infty}^{\phi} e^{-\tau'(\phi_0)}\sin\theta'(\phi_0)d\phi_0 \quad \text{for } -\infty < \phi < +\infty \tag{2.16}$$

By substituting (2.16) into (2.13), an integro-differential equation is created and it is solved numerically.

3. Numerical procedure

In this section, we describe numerical approach for the nonlinear problem derived in previous section. This numerical procedure has been successfully used by B. J. Binder [9], P. Guayjarernpanishk [15] and others for solving nonlinear integral equations. Firstly, the free surface must be truncated at ϕ_1 and ϕ_N for the corresponding far upstream $x \longrightarrow -\infty$, and far downstream $x \longrightarrow +\infty$, respectively. The truncated free surface is then discretized into N equally segments with

$$\phi_I = \left[\frac{-(N-1)}{2} + (I-1)\right]\Delta, I = 1, ..., N, -\infty < \phi < +\infty \tag{3.1}$$

and the unknown variables on the free surface are

$$\theta_I = \theta(\phi_I), I = 1, ..., N.$$

Here $\Delta > 0$ is the mesh spacing. We evaluate the values $\tau'(\phi_0)$ at the midpoints

$$\phi_M = \frac{\phi_{I+1} + \phi_I}{2}, I = 1, ..., N-1 \tag{3.2}$$

by applying the trapezoidal rule to the integral in (2.12) with summations over ϕ_I such that ϕ_0 is the midpoints. We evaluate $y_I = y(\phi_I)$ and $x_I = x(\phi_I)$ by applying the Euler's method and by using (2.14). This yields

$$\begin{cases} y_1 = 1 \\ y_{I+1} = y_I + \Delta e^{-\tau_M} \sin\theta_M, I = 1, ..., N-1 \end{cases}$$

and

$$\begin{cases} x_1 = 0 \\ x_{I+1} = x_I + \Delta e^{-\tau_M} \cos\theta_M, I = 1, ..., N-1. \end{cases}$$

Here $\theta_M = \dfrac{\theta_{I+1} + \theta_I}{2}$. We now satisfy (2.13) at the midpoints (3.2). This yields N non-linear algebraic equations for the N unknowns $\theta_I, I = 1, ..., N$. The derivative, $\dfrac{\partial\theta'}{\partial\phi}$, at the mesh points (3.1), is approximated by a finite difference, whereby

$$\frac{\partial\theta'}{\partial\phi} = \frac{\theta_{I+1} - \theta_I}{\Delta}, I = 1, ..., N-1.$$

The system of N equations with N unknowns is solved by Newton's method.

4. Presentation of results and discussion

The numerical procedure of section 3 is used to compute solutions for free surface flows over a successive triangular obstacles. For simplicity, we assume that the triangles are isosceles forming the angles $\gamma_i, i = 1, ..., m-2$ with the horizontal (see Figure 1). Also, we choose $\phi_{A_{\frac{m}{2}}} = 0$. Most of the calculations in this paper are obtained with $N = 401$ and $\Delta = 0.15$. For a given values of ϕ at the points $A_i, i = 1, .., m-1$, we compute waveless solutions for various values of the angles γ_i, Froude number Fr and the inverse Weber number δ. We denote by $L = \left|\phi_{A_{i+1}} - \phi_{A_i}\right|, i = 1, ..., m-2$ which represents

the length of the sides of the triangles. The problem is essentially characterized by four parameters; The Froude number Fr, the inverse of Weber δ, $|\gamma_i|$ and L. In supercritical ($Fr > 1$) or subcritical flow ($Fr < 1$) and a fixed values of $L = 2.5$ and $|\gamma_i| = \frac{\pi}{4}$, the effect of surface tension on the shape of free surface, is shown in Figures 4 and 5. It should be noted that the free surface elevation increases when the inverse Weber number δ decreases. The Figures 6 and 7 show the effect of the Froude number Fr for fixed values of $\delta = 0.5$, $|\gamma_i| = \frac{\pi}{6}$ and $L = 3$. It can be seen that the elevation of the free surfaces increases as Froude number Fr increases. When the surface tension is neglected ($\delta = 0$) and $Fr \to \infty$ (without gravity) and for an arbitrary values of δ and γ_i; the problem has an exact solution that can be computed via the streamline method due to Kirchhoff [2], in this case, the elevation of free surfaces reaches its maximum. The effect of varying the length L, whilst γ_i, δ and Fr are fixed is shown in Figure 8. Figure 9 illustrates the effect of varying the angles γ_i where $\delta = 0.7$ and $Fr = 2$ are fixed.

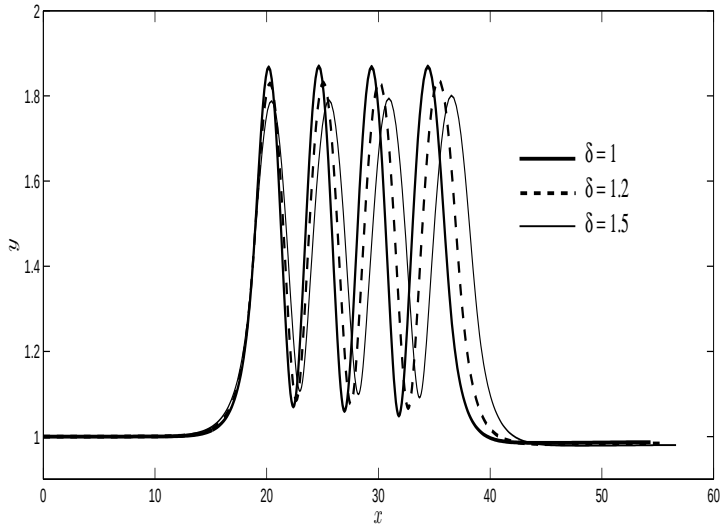

Figure 4. The shapes of free surface for $Fr = \infty, |\gamma_i| = \dfrac{\pi}{4}, L = 2.5$ and various values of the inverse Weber number δ.

5. Conclusion

In this paper, the problem of irrotational, two-dimensional free-surface flow over a successive obstacles has been presented. The fluid is assumed to be incompressible and inviscid. The fully non-linear problem is formulated by using a boundary integral equation technique. The numerical solutions are obtained, in the presence of surface tension and gravity. For supercritical flow ($Fr > 1$), there is a three-parameters family of solutions depending on the height of obstacle, the inverse Weber number δ and the Froude number Fr which is similar to the case of subcritical flow ($Fr < 1$). We have seen the effect of surface tension on free surface profiles for supercritical and subcritical flows. It noted that when the inverse Weber number decreases or the Froude number increases , the free surface elevation increases. The same observation is made when γ_i or L decreases the elevation of the free surface decreases and vice versa. The maximum free-surface elevation is obtained in the absence of

the surface tension and gravity, in this case, the exact solution can be found via the hodograph transform due to Kirchhoff [2].

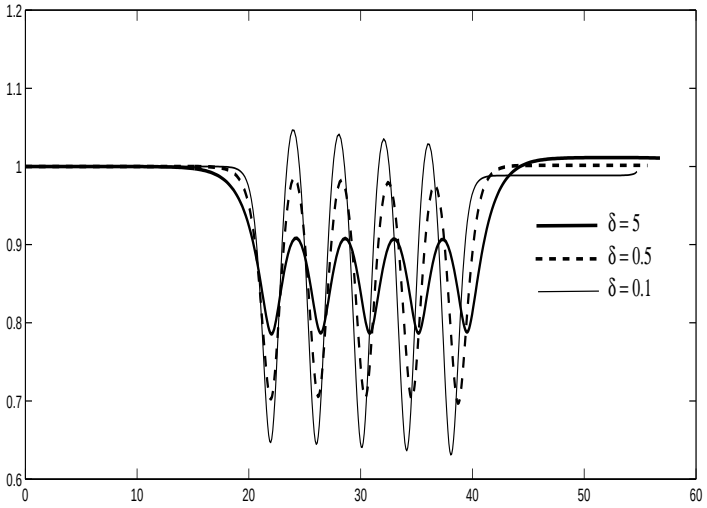

Figure 5. The shapes of free surface for $Fr = 0.8, L = 2.5, |\gamma_i| = \dfrac{\pi}{4}$ and various values of the inverse Weber number δ.

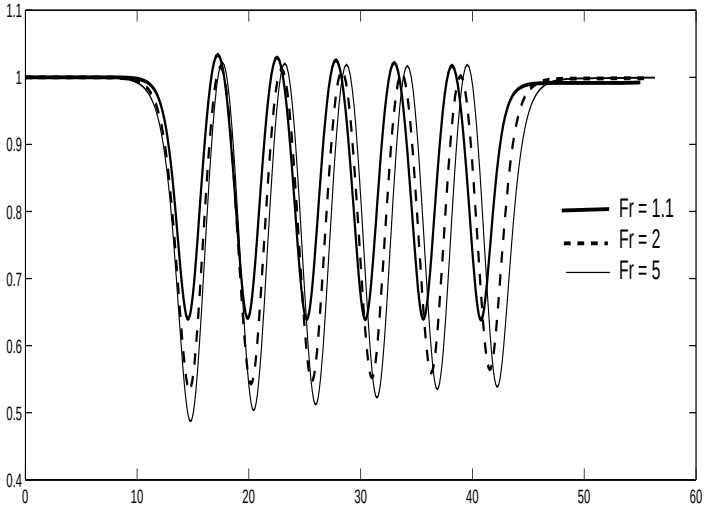

Figure 6. The shapes of free surface for $\delta = 0.5, L = 3, |\gamma_i| = \dfrac{\pi}{6}$ and various values of the Froude number Fr.

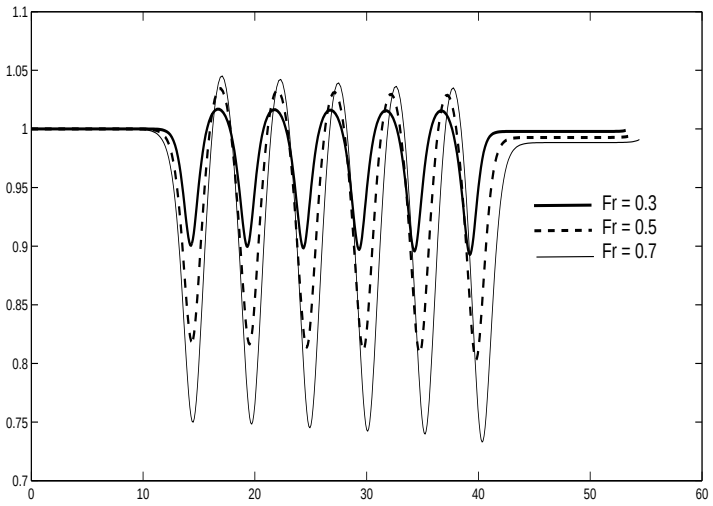

Figure 7. The shapes of free surface for $\delta = 0.5, L = 3, |\gamma_i| = \dfrac{\pi}{6}$ and various values of the Froude number Fr.

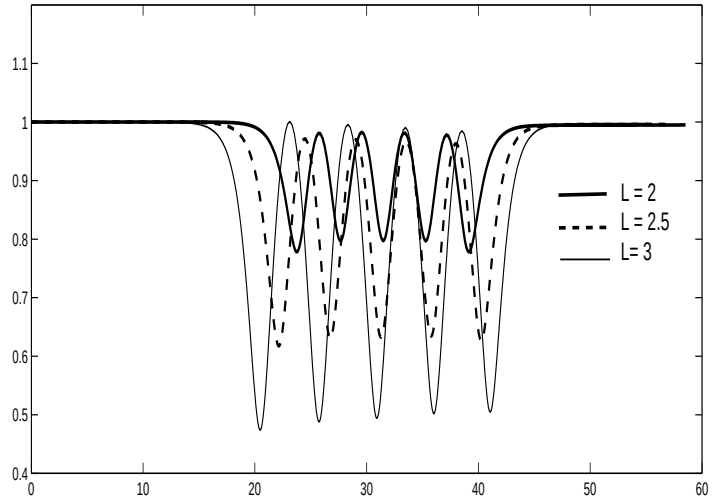

Figure 8. The shapes of free surface for $\delta = 1, Fr = 1.5, \phi_{A_6} = 0, |\gamma_i| = \dfrac{\pi}{4}$ and various values of the length L ($L = 2, L = 2.5, L = 3$) (from top to bottom).

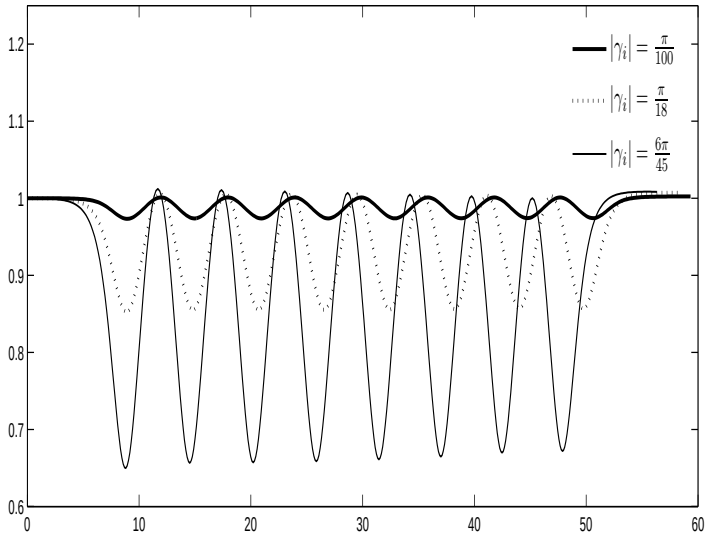

Figure 9. The shapes of free surface for $\delta = 0.7, Fr = 2, L = 3$ and various values of the angles γ_i where $|\gamma_i| = \frac{\pi}{100}, \frac{\pi}{18}, \frac{6\pi}{45}$ (from top to bottom).

Conflict of interest

The authors declare no conflicts of interest in this paper.

References

1. M. B. Abd-el-Malek, S. N. Hanna and M. T. Kamel, *Approximate solution of gravity flow from a uniform channel over triangular bottom for large Froude number*, Appl. Math. Model., **15** (1991), 25–32.
2. G. K. Batchelor, *An Introduction to Fluid Dynamics*, Cambridge University Press, 1967.
3. S. R. Belward, *Fully non-linear flow over successive obstacles: Hydraulic fall and supercritical flows*, J. Austral. Math. Soc. Ser. B, **40** (1999), 447–458.
4. S. R. Belward and L. K. Forbes, *Fully non-linear two-layer flow over arbitrary topography*, J. Eng. Math., **27** (1993), 419–432.
5. B. J. Binder, *Steady two-dimensional free surface flow past disturbances in an open channel: Solutions of the Korteweg-De Vries equation and analysis of the weakly nonlinear phase space*, Fluids, **4** (2019), 24. Available from: `https://www.mdpi.com/2311-5521/4/1/24`.
6. B. J. Binder, M. G. Blyth and S. W. Mccue, *Free-surface flow past arbitrary topography and an inverse approach for wave free solutions*, IMA J. Appl. Math., **78** (2013), 685–696.
7. B. J. Binder, F. Dias and J. M. Vanden-Broeck, *Influence of rapid changes in a channel bottom on free surface flows*, IMA J. Appl. Math., **73** (2008), 254–273.

8. B. J. Binder, F. Dias and J. M. Vanden-Broeck, *Steady free surface flow past an uneven channel bottom*, Theor. Comput. Fluid Dyn., **20** (2006), 125–144.
9. B. J. Binder, J. M. Vanden-Broeck and F. Dias, *Forced solitary waves and fronts past submerged obstacles*, Chaos, **15** (2005), 037106.
10. F. Dias and J. M. Vanden-Broeck, *Generalised critical free surface flows*, J. Eng. Math., **42** (2002), 291–301.
11. F. Dias and J. M. Vanden-Broeck, *Open channel flows with submerged obstructions*, J. Fluid. Mech., **206** (1989), 155–170.
12. L. K. Forbes, *Free-surface flow over a semicircular obstruction, including the influence of gravity and surface tension*, J. Fluid. Mech., **127** (1983), 283–297.
13. L. K. Forbes and L. W. Schwartz, *Free-surface flow over a semicircular obstruction*, J. Fluid. Mech., **114** (1982), 299–314.
14. S. Grandison and J. M. Vanden-Broeck, *Truncation approximations for gravity-capillary free surface flows*, J. Eng. Math., **54** (2006), 89–97.
15. P. Guayjarernpanishk and J. Asavanant, *Free-surface flows over an obstacle: Problem revisited*, In: Bock H., Hoang X., Rannacher R., Schlöder J. Editors, *Modeling, Simulation and Optimization of Complex Processes*. Springer, Berlin, Heidelberg, (2012), 139–151.
16. S. N. Hanna, *Influence of surface tension on free surface flow over a polygonal and curved obstruction*, J. Comput. Appl. Math., **51** (1994), 357–374.
17. R. J. Holmes and G. C. Hoking, *A note on waveless subcritical flow past symmetric bottom topography*, Euro. J. Appl. Math., **28** (2016), 562–575.
18. R. J. Holmes, G. C. Hoking, L. K. Forbes, et al. *Waveless subcritical flow past symmetric bottom topography*, Euro. J. Appl. Math., **24** (2013), 213–230.
19. A. C. King and M. I. G. Bloor, *Free-surface flow of a stream obstructed by an arbitrary bed topography*, Q. J. Mech. Appl. Math., **43** (1990), 87–106.
20. C. Lustri, S. W. Mccue and B. J. Binder, *Free surface flow past topography: A beyond-all-orders approach*, Euro. J. Appl. Math., **23** (2012), 441–467.
21. A. Merzougui and A. Laiadi, *Free surface flow over a triangular depression*, TWMS J. App. Eng. Math., **4** (2014), 67–73.
22. R. Pethiyagoda, T. J. Moroney and S. W. Mccue, *Efficient computation of two-dimensional steady free surface flows*, Int. J. Numer. Meth. Fluids, (2017), 1–20.
23. L. J. Pratt, *On non-linear flow with multiple obstructions*, J. Atmos. Sci., **41** (1984), 1214–1225.
24. J. M. Vanden-Broeck, *Gravity-Capillary Free Surface Flows*, New York: Cambridge University Press, 2010.

AIMS Press